This is the Pre-Published Version.

Z. Nan, M.A. Orabi, X. Huang, Y. Jiang, A. Usmani (2023) *Structural-fire Responses Forecasting via Modular AI*, **Fire Safety Journal**, 140, 103862. https://doi.org/10.1016/j.firesaf.2023.103863

Structural-fire Responses Forecasting via Modular AI

Zhoujun Nan[a], Mhd Anwar Orabi[a*], Xinyan Huang[a*], Yaqiang Jiang[b], Asif Usmani[a]

[a]*The Hong Kong polytechnic University, Hung Hom, Hong Kong, China*

[b]*Sichuan Fire Research Institute, Ministry of Emergency Management, Chengdu, Sichuan, China*

Corresponding to mhd-anwar.orabi@polyu.edu.hk (MAO), xy.huang@polyu.edu.hk (XH)

Highlights:

- Modular AI system is effective in structural-fire response forecasting
- 960 fire scenarios designed for training AI for an aluminium reticulated structure
- Individual AI models are LSTM RNNs for predicting displacement at local points
- Modular design makes system flexible & adaptable, improving accuracy & reliability

Abstract:

This study analyses the structural response of an aluminium reticulated roof structure that is constructed at Sichuan Fire Research Institute (Sichuan, China), and to be tested in fire. The structural fire behaviour under 960 localised fire scenarios is considered first, and then used to construct a database for training a modular artificial intelligence (AI) system for real-time forecasting. The system consists of several AI models, each of which predicts the displacement at a specific monitoring point. These individual predictions are then combined to generate a comprehensive forecast of the global structural-fire behaviour. The individual AI model utilized is a Long Short-Term Memory Recurrent Neural Network (LSTM RNN). The modular design allows different models to be modified or added as needed, making the system flexible and adaptable, and improving the accuracy and reliability of the predictions. The results demonstrate the effectiveness of the modular AI approach in accurately forecasting fire-induced structural collapses as indicated by the sensitivity the local models can have. The key objective of this research is to help to make informed decisions and prioritize efforts to minimize the risk of structural collapse in fire.

Keywords: *structural response; real time; artificial intelligence; RNN; LSTM*

1. Introduction

Fire-induced structural collapses are catastrophic events that can have dire consequences, including loss of life and property damage. With the erection of high-rise buildings, there have been several devastating fires [1–5] that caused the partial or progressive collapse of structures. For instance, the World Trade Center Towers fire (11 September 2001) [1] was a tragic event that had a profound impact on the field of structural fire engineering and even the world as a whole. A total of 2,996 people were killed in the attacks, fires and subsequent collapses, including both civilians and emergency personnel, as well as all the passengers and crew on the airplanes [6]. The economic impact could be upwards of a hundred billion dollars or more. That being said, however, structural-fire response is difficult to predict due to the unpredictable nature of fire, as well as the complex interactions between fire and structure. Structural collapse is also a major concern during firefighting and rescue operations. Fire-induced failure often presents warning signs that are not easily identifiable, leading to numerous firefighter fatalities over the years [6]. Traditional firefighting methods, predominately reliant on human communication, suffer from inaccurate modelling and slow communication systems, failing to incorporate real-time data to inform tactical interventions [7].

Computational fluid dynamics (CFD) and finite element method (FEM) are numerical modelling techniques that are commonly coupled to analyse the behaviour of structures under fire [8–14]. Nonetheless, due to the complexity of modern buildings and fire dynamics, structural fire analysis problems have become more nuanced [15] and identifying the worst possible fire scenario is still challenging [16,17]. Computer simulations are subject to limitations and uncertainties, including inaccuracies in the models used and limitations in the computational resources available, which obstruct their ability to be applied for real-time monitoring of structural fires. Today, PBD structural fire design relies heavily on the experience of engineers and their judgement, whether for fire scenario design, or prediction and assessment of structural response. Therefore, relying solely on design to reduce the risk of structural fire collapse is may result in an incomplete approach to fire safety [18]. This highlights the importance of developing accurate and reliable methods for predicting structural response in fire, and why the use of Artificial Intelligence (AI) is a promising area of research in this field.

Innovation in firefighting has led to various strategies, including the use of data analysis techniques for fire modelling and the deployment of sensors to monitor fires in real time. The FireGrid project [19] employed sensor data assimilation with ensemble prediction to achieve real-time forecasting of compartment fires, adapting techniques similar to those used in weather forecasting. More recently, the SureFire project introduced an amalgamation of Artificial Intelligence, Internet-of-Things (IoT), and Digital Twin technologies to aid smart firefighting, successfully identifying real-time fire scenarios in tunnels [20,21] and compartments [22,23]. The ability to forecast critical events bolsters urban infrastructure resilience to

fire hazards and elevates smart firefighting to be both reliable and practical [24]. The successful development of rapid forecasting technology for predicting structural failure during fires could significantly reduce risks to life and property. By providing emergency responders with key information about the stability of the structure, they can make informed decisions during their operations.

The integration of AI in fire and structural engineering is an actively researched topic [25]. Fu [26] proposed a machine learning (ML) framework for predicting the failure of steel framed structures in fire, using the Critical Temperature Method and incorporating Monte Carlo Simulation and Random Sampling to generate a dataset for training and testing.. Ye et al. developed an FE-based ML model framework to predict structural displacement based on temperature data obtained from the parametric fire model [27] or CFD [28]. It was demonstrated that Random Forest and Gradient Boosting models outperform the other models in terms of predictive accuracy. The use of Long Short-term Memory (LSTM) network is growing in popularity due to their ability to handle sequential data and make predictions based on long-term dependencies [29]. A real-time prediction method for fire-induced structural collapse was put out by Ji et al. [30] utilizing an LSTM network, which is based on key monitoring physical parameters [31]. Previous studies have primarily focused on the development of single, sophisticated ML models, which are trained on specific datasets and used to forecast structural behaviour under similar fire conditions. It is difficult to apply to different types of structures. These models can be complex, Inflexible, and lack interpretability. Additionally, these models can lead to inaccurate discriminatory predictions if the data contains any biases or imbalances.

In this paper, modular AI approach is proposed of real-time forecasting of the behaviour of an aluminium roof structure that will be tested until collapse in fire. Modular AI refers to the use of modular, specialized artificial intelligence models to address specific tasks within a larger problem, rather than relying on a single, monolithic AI model. The paper starts by introducing the roof structure, presenting the 960 localised fire scenarios used for data generating, and then discussing the development of Modular AI models.

2. The Structure and Future Experiment

To investigate the fire-induced progressive structural collapse, an aluminium reticulated roof structure has been constructed in Sichuan Fire Research Institute. The structure, depicted in Fig. 1, measures 10 m in length, 7.2 m in width, and 8 m in height, and is pinned to a concrete supporting frame. The roof is composed of rigidly connected I cross-beams 175×80×5×8 ($H \times B \times t_w \times t_f$ in mm) made of EN AW-6061-T6 aluminium. The loads equivalent to a glass façade were applied to the connections, ranging from 0.92 kN to 2.21 kN, as shown in Fig. 1(c).

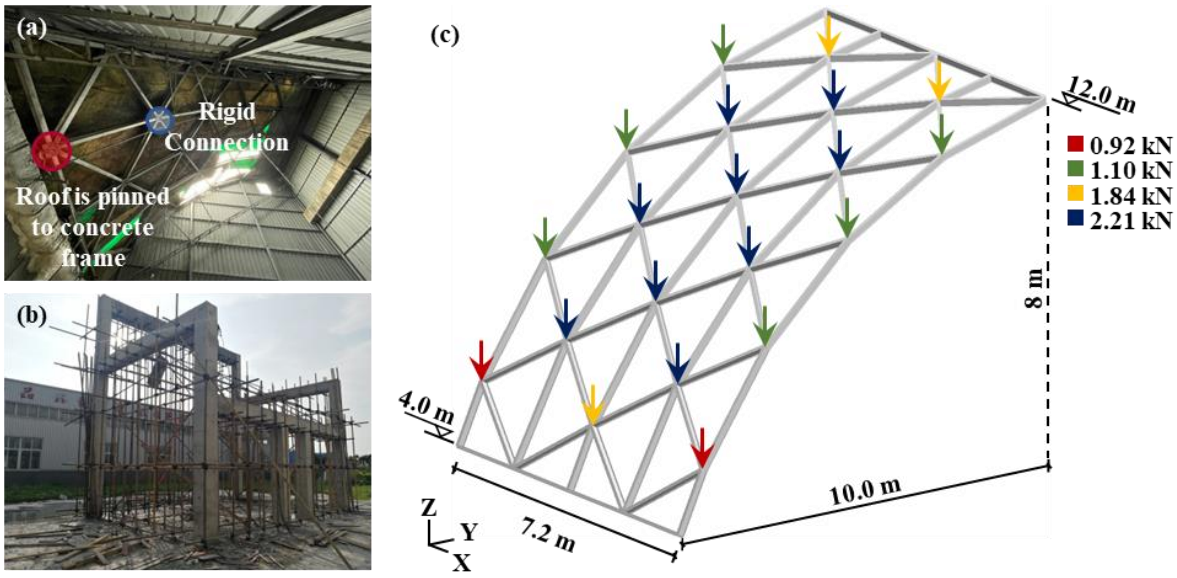

Fig. 1 Details of the test structure: (a) connection classifications; (b) supporting concrete frame; and (c) dimensions and imposed load.

The structural fire test will examine the behaviour of a "slice" of aluminium reticulated roof for an exhibition centre. Piles of wooden cribs will be utilized as fire load, resulting in a 24 MW fire that will last approximately 30 minutes. The fuel load density, calculated over a floor area of 72 square meters, is equivalent to 600 MJ/m^2 [32] and is consistent with the prescribed standards for fuel-controlled fire with sufficient ventilation, which is typical of fires in large open spaces. The elevated fire intensity is designed with the expectation of triggering the progressive collapse of the structure. This test will not only provide valuable insights into the structural response to fire, but also serve as a platform to evaluate the effectiveness of the integrated fire safety system, including smart fire service devices, a digital twin, real-time monitoring, and rapid forecasting.

3. Numerical Models

3.1 FEM Structural Model

A finite element model of the roof was built in the Integrated Simulation Environment (ISE) and was analysed using OpenSees. Displacement-based beam-column elements with fibre-based sections were used to represent the beams of the roof. The number of integration points in the cross-section was 15. The boundary conditions of the roof structure were pinned at the supports and all the beam-to-beam connections were assumed rigid as in the experimental setup. The density, Young's modulus and yield strength of aluminium elements were taken to be 2700 kg/m^3, 70 GPa and 270 MPa, respectively.

Both the fire modelling and subsequent heat transfer analysis were also carried out using OpenSees within the ISE [33,34]. The gas temperatures generated from the design fire scenarios (as outlined in Section 5.4),

were used as the fire boundary input for the 2D heat transfer analysis in OpenSees for fire. A series of heat transfer analyses for a subset of fire configurations was performed. It was found that the thermal thinness of the aluminium structural members meant that the gas temperatures and solid temperatures were in steady state heat transfer almost from the beginning of the fire. Therefore, it was concluded that the gas temperatures can be used directly as a uniform fire load in the FE structural model. The heat transfer analysis addresses transient governing equations, encompassing the contributions of convection, conduction, and radiation [35]. The output of thermal response, saved in a data file, consists of a set of coordinate points, facilitating subsequent thermos-mechanical analysis. The thermal properties of aluminium are defined according to Eurocode 9 [36]. It should be noted that the fire load was not applied to the joists, which are the horizontal structural members shown in **Fig. 1**(c), in the numerical model. This is due to the fact that the joists are fixed and provide mainly stiffness, and are not expected to significantly impact the structural behaviour in real fires. However, it should be considered that if the joists in the lower part of the roof were at high temperature in the model, they would experience significant deformation and buckle early on, which could affect the simulation.

A mesh-sensitivity analysis was conducted to investigate the impact of element size on simulation accuracy. For illustrative purposes, the structure subjected to the design localised fire scenario Case 219 (see **Section 3.2**) was chosen as an exemplar. This scenario pertains a 30 MW fire localised at Location 3 (middle center) under the roof, as delineated in **Fig. 3**. Three alternative mesh densities, consisting of 4, 8, and16 elements for each member were considered for the beam. The displacement at monitoring point 4 (see **Fig. 7**(b)) is displayed in **Fig. 2**. As evidenced by the data presented in **Fig. 2**, the structural response showed little sensitivity to changes in mesh size at elevated temperatures, especially before the occurrence of buckle and collapse. Accordingly, for maximum computational efficiency, each member was discretized with 8 elements, resulting in a total of 552 elements modelling 69 structural members.

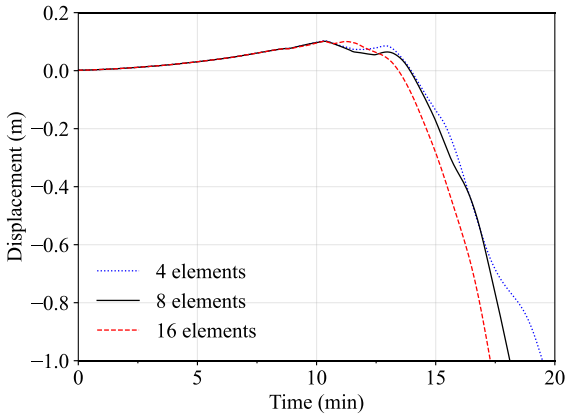

Fig. 2 Comparison of displacements at displacement monitoring point 4 for various mesh densities.

In addition to mesh size, sensitivity analysis was also performed on the scaling of analysis time. In dynamic analysis of the structural response to fire, it is common to scale down the real time in the model to account for the quasi-static nature of the problem [18,37,38]. However, this approach can introduce significant inertia forces to the system due to the faster application of the load, which my impact he structural response. Hence, an appropriate time scale for a dynamic analysis of the structural response to fire is required to be determined first. In this study, it was shown that the duration of fire can be scaled by a time factor of 1/1000 for the implicit dynamic analysis in OpenSees. The step size was 0.001s, and the total analysis time was set to 1.8 s.

The static interval used load-controlled integration with the Band General system of equations, the reverse Cuthill-McKee (RCM) numberer, transformation constraints handler, and the Full Newton-Raphson algorithm. The transient interval used load-controlled integration with the UmfPack system of equations, the RCM numberer, transformation constraints handler, the Krylov Newton algorithm, and performed the integration with the Newmark method with the average acceleration method ($\gamma = 0.5,\ \beta = 0.25$) as recommended by Orabi et al. [39].

The analysis produces quasi-static responses prior to the buckling of the heated beams, followed by dynamic responses. Meanwhile, Rayleigh damping was applied with nominal mass and stiffness damping coefficients of 0.05 and 0.005 [39], respectively, for numerical stability. However, it should be noted that Rayleigh damping is not commonly used to model the response of structures under fire due to the differences in damping properties at high temperatures. This issue will be further discussed in future research. In some of the cases, mass scaling with a factor of 10 was implemented in the finite element analysis. The mass scaling method artificially increased the mass of elements by a magnitude of ten, thereby enhancing the stability of the computational model. The application of mass scaling was judiciously executed, with careful consideration of its potential impact on the stability and accuracy of the simulation outcomes.

3.2 Fire Scenarios

The Hasemi's localised fire model [40] was applied in the design of localised fire scenarios in this study. Regarding the uncertainty of fire, two fire-related input parameters considered were the fire sizes and fire locations. The parameters were varied systematically to generate a comprehensive and representative set of 960 fire scenarios. To efficiently create design fire scenarios, we developed Python scripts to integrate with the natural fire model [41], enabling automated generation. This process minimizes manual errors and enhances efficiency. The natural fire model, developed by the author, allows for increased design flexibility by permitting the input of spatial fire location and various fire sizes via an external file.

The eighty fire sizes ranged from 0.5 MW to 40 MW with an interval of 0.5 MW as detailed in **Table 1**. The 0.5 MW fire scenario represented a small and controlled fire in a residential or commercial building. The 40 MW fire scenario represented extreme conditions that are rarely encountered in buildings with common occupancy types. The twelve fire locations highlighted in **Fig. 3**. Each fire location was directly under the mid-span of the corresponding beam. The parameters related to the fire scenarios were specified in accordance with common design practices [32,42,43]. The fuel load density on the floor area was set at a maximum of 1000 MJ/m^2, with a heat release rate per unit area (HRRPUA) 1000 kW/m^2. The fire growth rate was determined as "fast" (α value of 0.0469 kW/s^2), with a fire duration of 30 minutes.

Table 1 Values for the different parameters of the localised fire scenarios.

Parameters of localised fire scenarios	**Values**
Fire location (see **Fig. 3**)	Loc.1 (bottom centre), Loc.2 (lower centre), Loc.3 (middle centre), Loc.4 (upper centre), Loc.5 (top centre), Loc.6 (lower right), Loc.7 (upper right), Loc.8 (middle right edge), Loc.9 (top right conner), Loc.10 (lower left), Loc.11 (middle left), Loc.12 (upper left)
Fire size (MW)	0.5, 1.0, 1.5, 2.0, 2.5, … 38.0, 38.5, 39.0, 39.5, 40.0 (ranged from 0.5 MW to 40.0 MW with an interval of 0.5 MW)

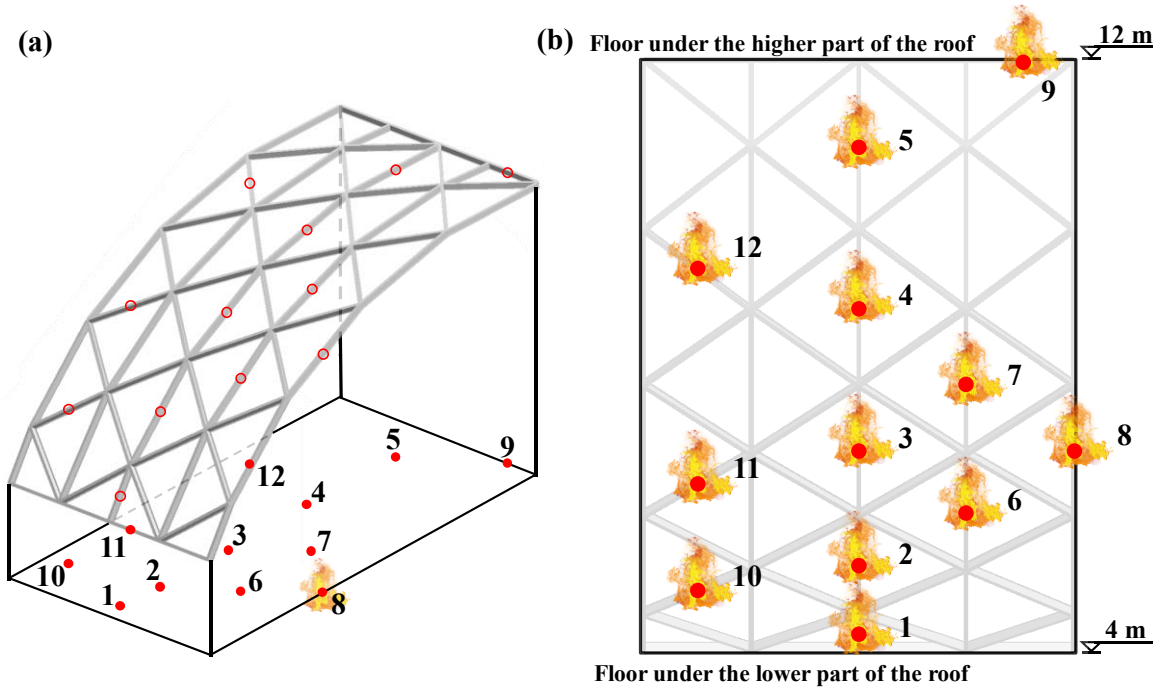

Fig. 3 Selected fire locations on the floor: (a) schematic; and (b) top view with the projection of the roof.

Fig. 4 and **Fig. 5** show the effect of fire location and fire size, respectively, on the temperature distribution at the level of the roof. Because of the curvature of the structure, the ceiling height of the structure varies at different locations. As shown in **Fig. 4**, even with the same fire intensity (e.g., 30 MW), due to different fire locations (e.g., bottom centre, middle right edge, and top right corner in this study), the temperature fields are significantly different. **Fig. 5** shows that, as expected, the larger the fire size, the higher the temperature. This is particularly the case directly above the fire source. The increase in fire sizes also results in a larger area of the structure being significantly affected by the fire.

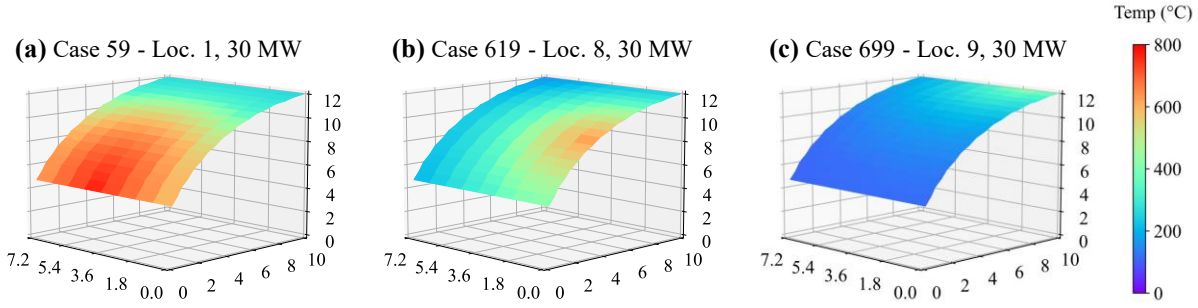

Fig. 4 A sample of three cases considering different localised fire locations with the same fire intensity of 30 MW: (a) Case 59 - Loc.1 (bottom centre); (b) Case 619 - Loc.8 (middle right edge); and (c) Case 699 - Loc.9 (top right corner).

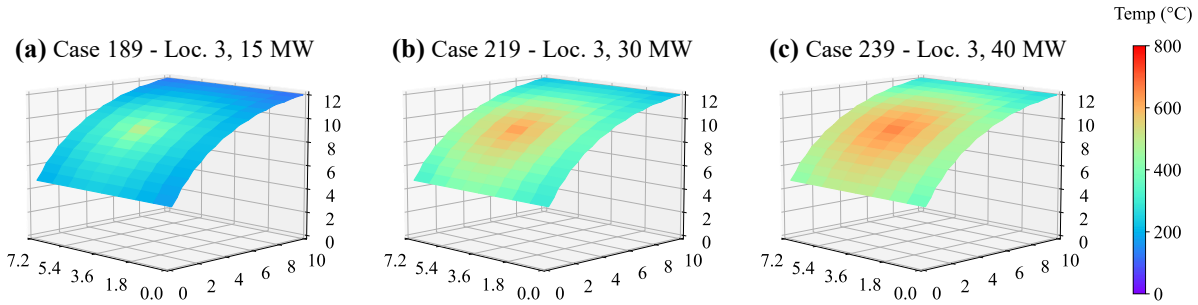

Fig. 5 A sample of three cases considering different localised fire intensities at the same fire location Loc.3 (middle centre): (a) Case 189 - 15 MW; (b) Case 219 - 30 MW; and (c) Case 239 - 40 MW.

4. Structural-fire Responses

When the roof is subjected to localised fire, the patterns of structural response are presented in **Fig. 6**. Typically, the heat generated by the fire induces thermal expansion and results in an upward deflection of the roof. If the fire is not suppressed at an early stage, the softening of structural members may cause buckling, leading to a loss of strength and stability. In certain situations, the fire is naturally extinguished, and the structural response reaches a halt before any severe structural damage occurs. However, in cases of intense fires, it can lead to buckling, deformation, and ultimately, collapse of the structure. The partial

collapse and global collapse can be observed, as evidenced by large but controlled deflections and runaway deflections, respectively. The structural responses in a fire are usually nonlinear and time-dependent, as the structure undergoes significant changes in behaviour over the course of the fire. It is imperative to consider the effect of localised failure, especially the failure of key structural components, on the global structural responses.

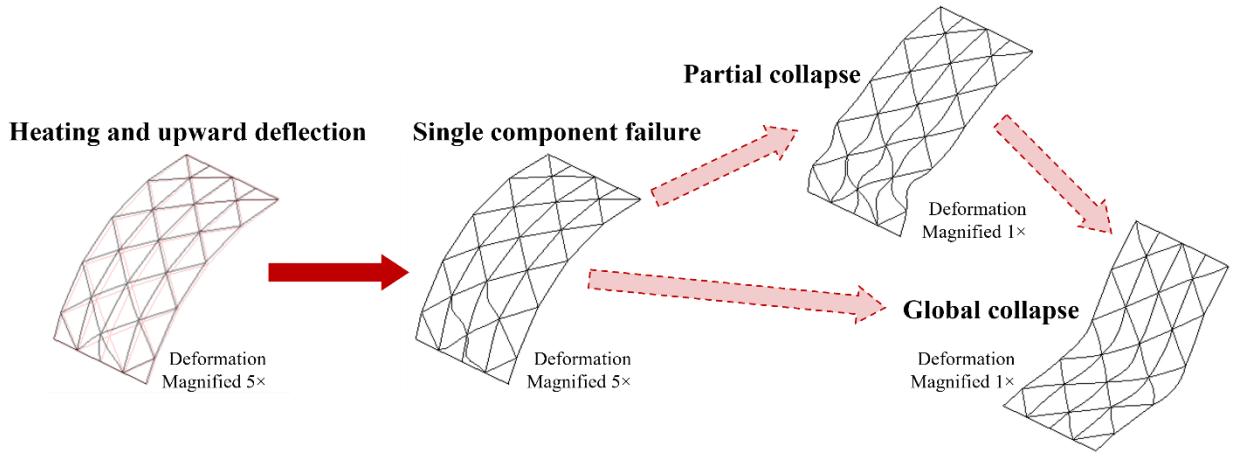

Fig. 6. The pattern of structural responses under localised fire.

Fig. 7 depicts the twenty-one monitoring points dispersed across the roof, chosen to observe structural responses under the non-uniform gas-phase temperature distribution. Data pertaining to gas temperature was gathered from thirteen points at ceiling height, as identified in **Fig. 7**(a). Corresponding to critical connection locations, displacements were recorded at eight monitoring points as indicated in **Fig. 7**(b). The aggregated dataset, inclusive of gas temperature and displacements from the selected monitoring points, also served as the initial data for creating a database for modular AI training, as detailed in **Chapter 5**.

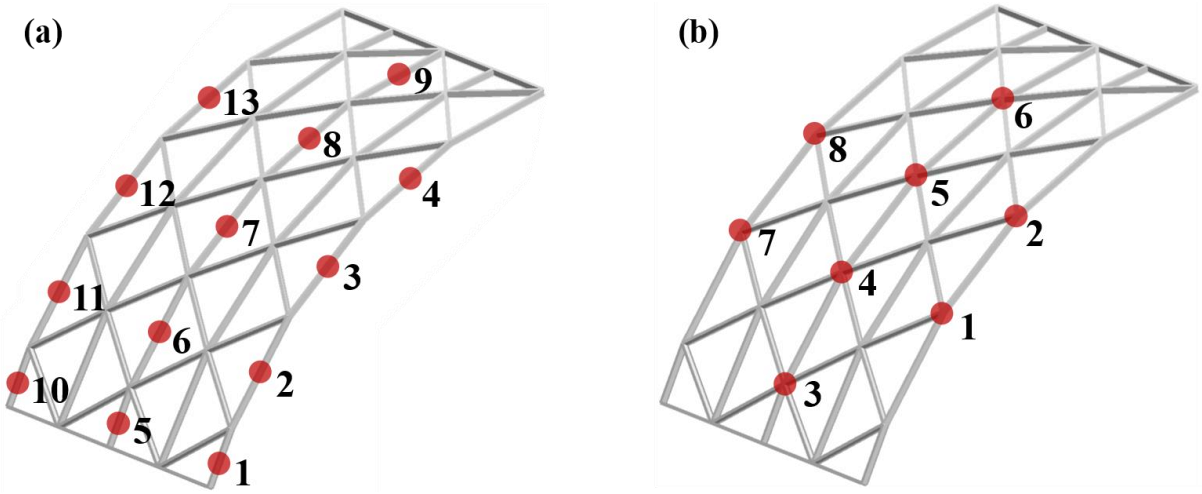

Fig. 7 Monitoring points: (a) temperature; and (b) vertical displacement.

4.1 Single Member Buckling

Fire-induced heat can trigger a series of structural reactions, primarily the expansion of structural beams and a simultaneous reduction in the strength of their materials due to softening, both of which can led to the buckling of structural members. Eurocode [36] states that aluminium loses nearly 45% of its proof strength at 250 °C, completely diminishing at 550 °C.

In localised fire Case 607, a 24 MW fire is positioned at Loc. 8, under the middle right edge of the roof (refer to **Fig. 3**). As depicted in **Fig. 8**(a), the maximum gas-phase temperature recorded at the gas temperature monitoring point 3 (which is directly above the fire source) was 585 °C, surpassing the critical 550 °C threshold. However, surrounding monitoring points captured lower peak gas temperatures, such as 446 °C, 398 °C and 308 °C at point 2, 4, and 7 respectively. This demonstrates the limited affection of the 24 MW fire at Loc.8 on the roof.

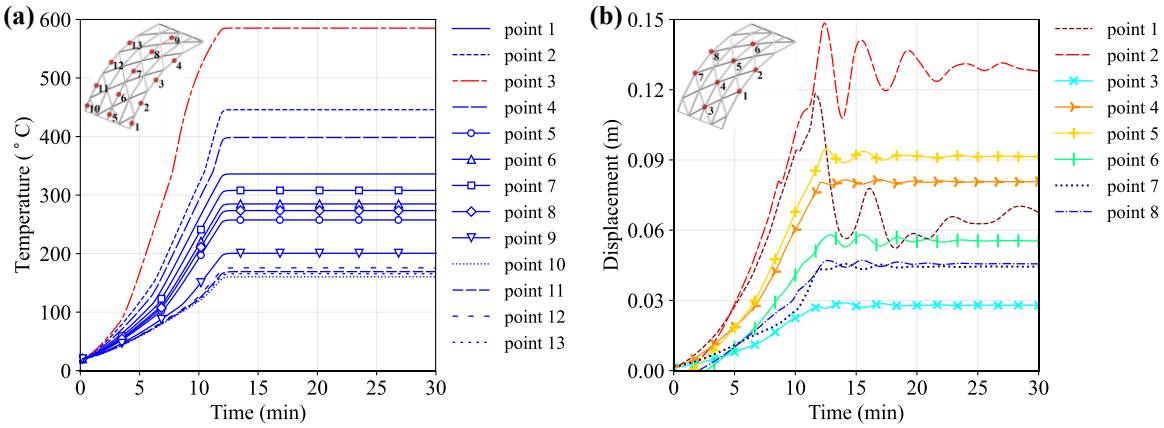

Fig. 8 Expected behaviour for localised fire Case 607: (a) gas temperatures at the different monitoring points; and (b) displacements of the displacement monitoring points.

In Case 607, only a certain range of the aluminium beams were exposed to high thermal loads (e.g., 550 °C), potentially pushing them to failure. **Fig. 9** reveals that longer, inclined beams located at the lower, closer-to-fire sections of the roof were the first to buckle. Multiple factors account for this, including the closer proximity to the fire source and consequent exposure to higher thermal loads. Moreover, the structural members close to the roof's fixed end experienced unfavourable conditions due to increased compression forces, along with the upward roof deflection caused by heating-induced expansion. Despite the buckling of several members, the overall structure endured the fire, as evidenced in **Fig. 8**(b). The compromised beams only caused a slight fall of displacement monitoring points 1 and 2, as shown in **Fig. 8**(b). This study classifies such a structural fire response as "single member buckling", where the structure withstands the fire despite several members buckling, and none of the displacement monitoring points exceeds the critical

displacement, -0.5 m. This critical displacement is roughly equivalent to L/20, with L representing the structure's 10 m span.

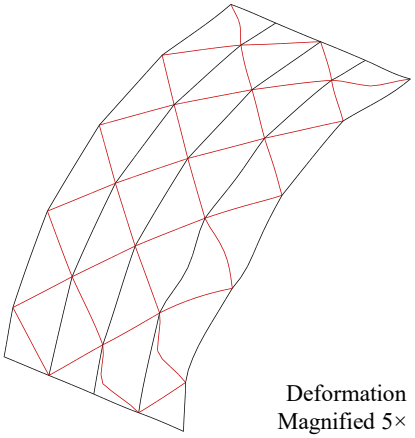

Fig. 9 Structural deformation featuring beam buckling in Case 607, observed after 14 minutes of exposure to localised fire.

4.2 Partial collapse

Demonstration Case 847 was selected to exemplify partial collapse under localised fire. In this case, the fire is positioned in the middle-left section on the floor beneath the roof (i.e., Loc.11 as depicted in **Fig. 3**), with a fire size of 24 MW. The fire size of 24 MW aligns with the experimental design fire scenario detailed in **Chapter 2**.

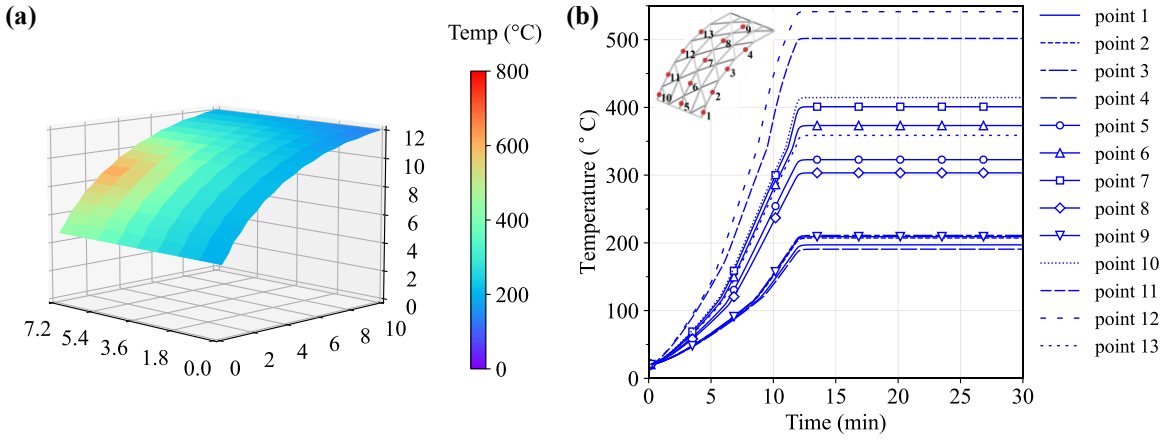

Fig. 10 Thermal load for localised fire Case 847: (a) gas temperature contours; and (b) gas phase temperature at monitoring points.

Thermal loads generated in Case 847 are represented in **Fig. 10**(a), where the gas temperature directly above the fire source peaked at 600 °C. However, further away from the ignition point, where the ceiling height

approximates 12 m, the gas temperature was lower 200 °C. As further indicated in **Fig. 10**(b), all gas temperatures measured from the thirteen monitoring points remained below 550 °C. This observation shows that even a relatively large fire does not homogeneously heat the entire roof structure. This heterogeneity of thermal impacts is likely amplified by the unique configuration of the roof, specifically its curved reticulated design and the differing ceiling heights. These features may limit the spread of heat, causing only localised sections of the ceiling to be affected by the fire.

Fig. 11 presents the structural responses of the roof under the localised fire scenario Case 847. A partial collapse is observable in **Fig. 11**(a) and is also identifiable in the time-displacement history of the monitoring points. As depicted in **Fig. 11**(b), the displacement at monitoring point 7 exceeded the critical value of -0.5 m after roughly 15 minutes of fire exposure. A sequential fall was recorded at monitoring point 8, with a displacement rate of 5 mm/s, indicating a partial collapse here. Despite the displacement at a few monitoring points exceeding -0.5 m towards the end of the simulation, the majority of the roof remained intact. Only some structural members demonstrated severe yet localised deflection, leading to a conclusion of partial collapse under localised fire Case 807. This observation demonstrates the robustness of the reticulated roof structure that may be attributed to the load redistribution. In reticulated roof structures, when certain members fail or buckle under stress (such as from a fire), the load they were bearing is transferred to the other members. This redistribution of loads can often prevent a complete collapse by allowing the structure to maintain its overall integrity, despite localised failures. Therefore, the ability of a reticulated structure to redistribute loads is a crucial factor in its resistance to collapse under severe conditions.

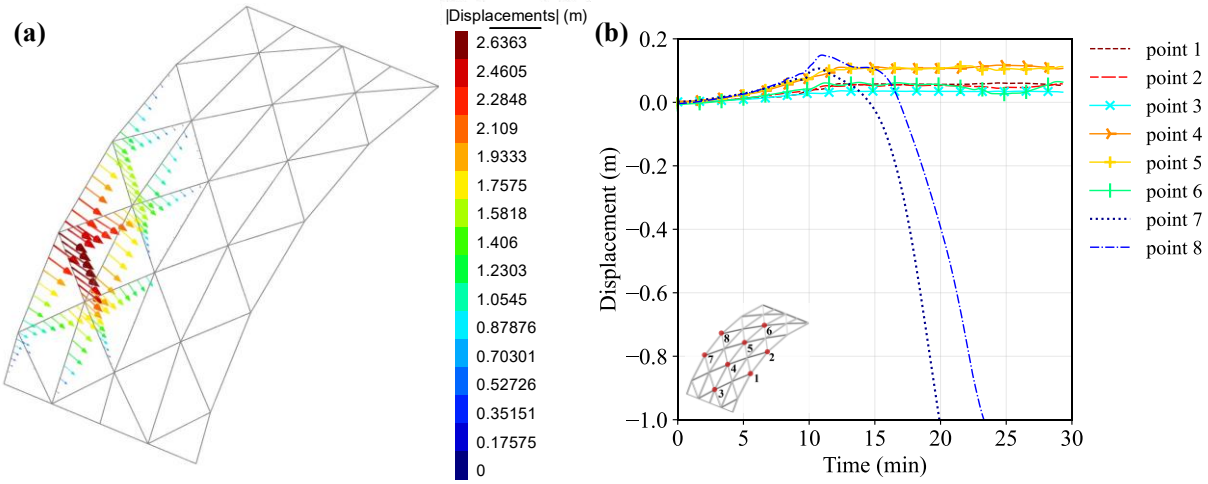

Fig. 11 Expected structural behaviour for localised fire Case 847: (a) displacement vectors, and (b) displacements at monitoring points.

4.3 Global collapse

In this section, localised fire scenario Case 127 has been selected to present a study of the significant thermal loads and consequential global structural collapse. **Fig. 12** represents the thermal and structural responses of the roof under a 24 MW localised fire which is positioned at the bottom center of the roof as illustrated in **Fig. 3**(a). The corresponding gas temperatures at the monitoring points for Case 127 are detailed in **Fig. 12**(a). It is noted that the gas temperature reached a peak of 681 °C directly above the fire source. This extreme temperature is indicative of the intense thermal stress exerted on the structural members in the immediate vicinity of the fire, possibly pushing them towards their material failure thresholds. While even at a distance, for instance at gas temperature monitoring point 9, the gas temperature still recorded a considerable 225 °C. This, in turn, resulted in a global collapse of the structure, a stark contrast to the partial collapses witnessed in other cases.

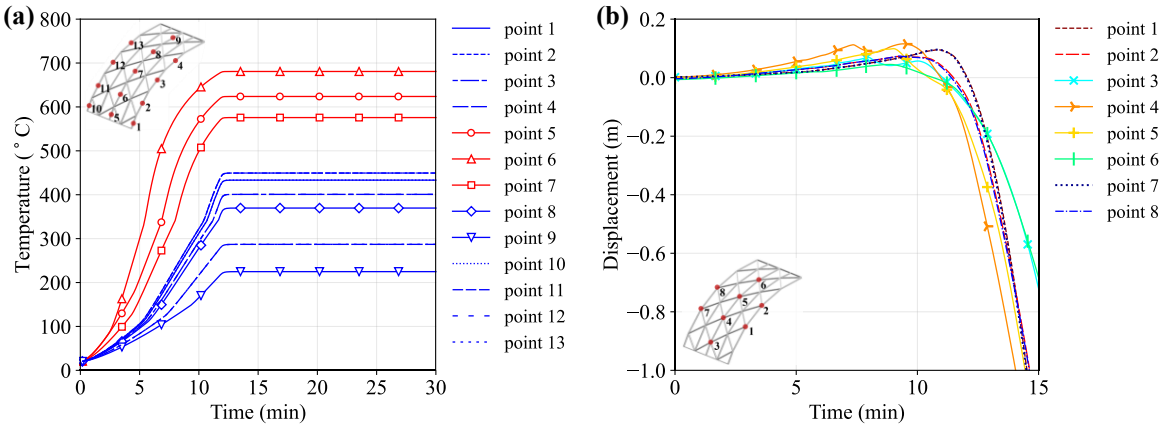

Fig. 12 Expected behaviour for localised fire Case 127: (a) gas temperatures at the different monitoring points; and (b) displacements of the displacement monitoring points.

The evidence for global collapse can be discerned from the time-displacement history of the displacement monitoring points, as depicted in **Fig. 12**(b). Here, it is noted that the displacement at all monitoring points exceeded the critical value of -0.5 m, and this occurred within approximately 13 minutes of fire exposure. The exceedance of the critical displacement value across all monitoring points reinforces the conclusion of a global rather than localised structural failure. This underscores the importance of considering a range of fire scenarios in structural fire analysis, particularly for structures with complex geometries like reticulated roofs.

4.4 Analysis of parametric studies

The structural responses of the reticulated roof structure under localised fire have been comprehensively analysed through the investigation of 960 design localised fire scenarios. In conclusion, this study provides

invaluable insight into the fire resistance of structures, highlighting the complex interplay of fire location, size, structure design, and material properties. The large number of fire scenario considered is expected to implicitly subsume any variations or uncertainty in the structure. By evaluating fire sizes changes at increments of 0.5 MW, it is expected that any structural behaviour that would appear due to weaker or stronger material properties, for example, would still appear in the database. However, the ability of the AI system to recognise these failure modes is expected to be slightly compromised as these uncertainties were not explicitly included in the simulation database.

We categorized the structural fire responses of the roof into three distinct failure modes: non-failure (no failure or "single member buckling"), partial failure (partial collapse), and failure (global collapse). This categorization is based on the premise that a critical displacement of -0.5 m signifies a significant structural response.

- A non-failure case, where the structure endures the fire, even with several members buckling, and none of the displacement monitoring points exceed the critical displacement of -0.5 m.
- A partial failure case is characterized by the displacement at several monitoring points exceeding the critical displacement towards the end of the simulation, even though the majority of the roof remains intact. Specifically, we classified scenarios as partial failure cases if a maximum of two points (i.e., 1 or 2 points) exceeded -0.5 m.
- A failure case is characterized by progressive collapse. However, we classified a situation as a global collapse if more than three points exceeded the critical displacement of -0.5 m, or if at least two points exceeded a large displacement of -1.0 m. This criterion provides a conservative judgment of global collapse. Given the roof is constructed of rigidly connected I-beams, if more than two points exhibit relatively larger displacements (e.g., the critical displacement -0.5 m or the large displacement -1.0 m), there is a high probability of triggering progressive collapse. Furthermore, we introduced the second condition to account for scenarios where numerical simulations might not converge and stop prematurely, due to the drastic fall of some points, before the end of the entire fire duration (30 minutes).

As shown in **Fig. 13**, the structural responses of the roof have a strong dependence on the location and intensity of the fire. The risk of collapse is significantly higher when the fire occurs under the lower part of the roof, as indicated by fire locations Loc.1, Loc.2 and Loc.10 (refer to **Fig. 3**). This phenomenon is primarily attributed to the intensified heat exposure experienced by these regions of the roof due to their proximity to the fire source. Such exposure subjects the nearby aluminium beams to extreme thermal loads, possibly propelling them towards their material failure thresholds. In addition to this, the structural members near the fixed end of the roof are subjected to unfavourable conditions. Heat-induced expansion,

coupled with upward deflection of the roof, leads to increased compressive forces, thereby escalating the risk of collapse. An intensive fire under these conditions could precipitate a sudden, progressive collapse without preceding indications, complicating real-time monitoring and rapid forecasting of fire-induced structural failures. This underscores the criticality of comprehensive fire location and size consideration in risk assessment and performance-based design.

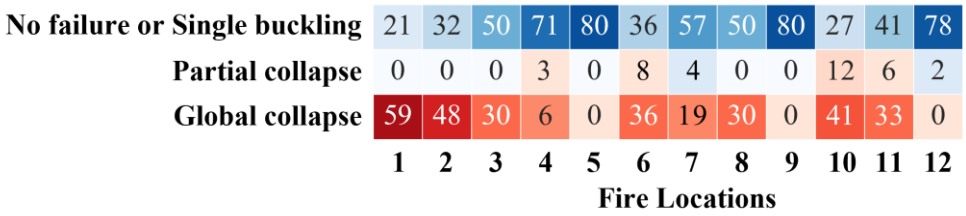

Fig. 13. Case statistics based on structural-fire responses.

Meanwhile, it is crucial to note that the specific load redistribution within the reticulated roof, and the consequent survival of portions of the structure, depend on a multitude of factors. These factors include the design and arrangement of the structural members, as well as the intensity and duration of the fire, as demonstrated in scenarios with different fire locations, depicted in **Fig. 13**. Specifically, the differential thermal impact of fire is likely accentuated by the unique configuration of the curved reticulated roof with variable ceiling heights. As shown in **Fig. 14**, an linear increase in fire size is required to trigger a global collapse as ceiling heights rise. Despite the formulation of 960 localized fire scenarios with 30 minutes of fire duration, more than 65% of cases resulted only in the "single member buckling" of structural members, if any failure occurred at all. This finding suggests that, in large space structures with elevated ceilings, fire impacts on the roof structure may not be as severe as typically anticipated in the prescriptive design.

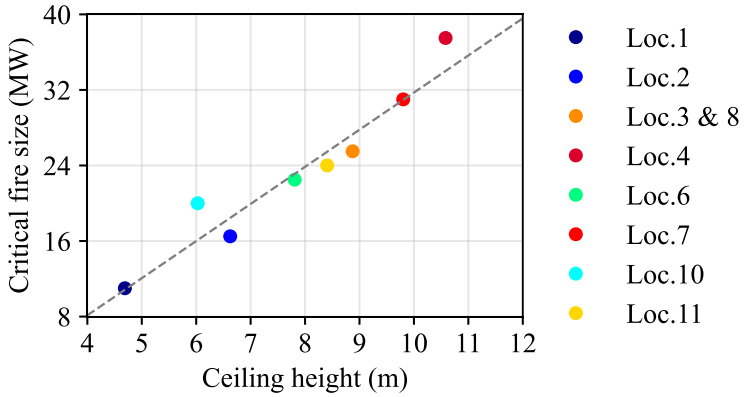

Fig. 14 Critical fire size required to induce global collapse in various fire locations with differing ceiling heights.

5. Generated Training Data

To effectively train a deep learning model, it is crucial to have a vast amount of data. The training database, consisting of fire temperatures and corresponding structural displacements, was generated using OpenSees. The process behind the generation of the database is illustrated in **Fig. 15**. The initial step involved creating a library of localised fire scenarios using the Hasemi's localised fire model [40]. Each scenario was unique in its "location" and "size", accounting for the potential spatiotemporal distribution of temperatures in reality. A subset of fire configurations underwent heat transfer analyses, revealing that the thermal thinness of aluminium structural members resulted in steady state heat transfer between the gas and solid temperatures almost immediately after the fire started. As a result, it was determined that the gas temperatures could be directly applied to the FE structural model as a uniform thermal load. Finally, the displacement at several crucial locations of the roof structure was extracted and incorporated in the databased.

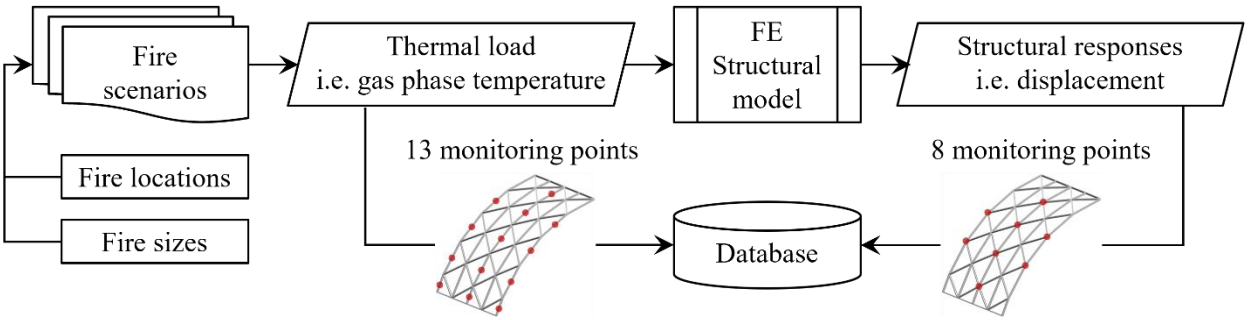

Fig. 15 Flowchart for the generation of training database.

As illustrated in **Fig. 15**, the data was collected from 21 monitoring points across the roof. The gas temperature data was obtained from 13 monitoring points at various ceiling height, refer to**Fig. 7**(a). The time series of gas temperature curves was scaled by a factor of 1/100, in accordance with the displacement data. Ensuring consistency in the data sequence is crucial in facilitating the ability of model to learn patterns in the data and generalized better to new unseen data. It is worth noting that the gas temperatures were only scaled for database generation purposes; the heat transfer analyses were still performed using the original time series. Displacements were recorded at 8 key connection locations, as shown in **Fig. 7**(b). The combination of gas temperature and displacement data at the selection monitoring points served as the starting point for database generation. Future iterations of this work may also consider incorporating additional information such as axial forces within individual members.

More detailed process involved in the generation of the database is depicted in **Fig. 16**. The first step in this process involved assigning thermocouples to the FEM structural model in ISE software (i.e., GiD+OpenSees). The thermocouples were used to link the structural model and design fire scenarios, and

served two main purposes to generate training data. With the assignment of thermocouples in the structural model, their spatial locations were determined, and they were set up as probes in .tcl files to capture the gas-phase temperature at specific locations generated by design fire scenarios. To effectively generate design fire scenarios, a natural fire model in OpenSees was applied. The natural fire model provided greater flexibility for designing fire scenarios and was incorporated with Python scripts for automated generation, reducing manual errors and improving efficiency. Thermocouples were also used to import gas temperature as thermal load to the structural model for heat transfer analysis. In this study, only one uniform thermal load was applied for each structural member, namely, the gas temperature differences along the length of the structural member were not considered. Hence, only one thermocouple was assigned to the mid-span of each structural member in this case, as shown in **Fig. 16**. To account for temperature distribution differences along the length of beams, additional thermocouples could be set up by dividing the beams in geometrical mode. This would allow for more accurate data collection. After heat transfer and subsequent structural analysis, the displacement and gas temperature at several crucial locations of the roof structure were extracted and incorporated in the database.

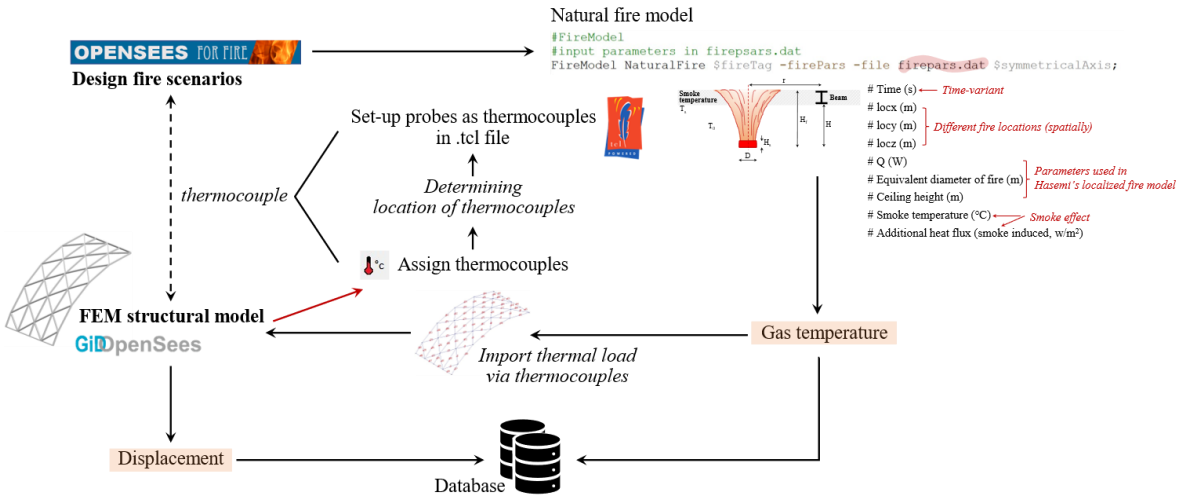

Fig. 16 Detailed process involved in the generation of the training database.

6. Modular AI Models

6.1 Methodology

Forecasting a time series using deep learning is usually achieved using recurrent neural networks (RNNs). In this type of network, each time step of the input sequence is fed recursively into the model so that the prediction of the next entry in the sequence is based on the history of the time series. Long-Short Term Memory (LSTM) RNNs are a special category of RNNs in which the nodes are enriched with more sophisticated gates that allow the network to selectively retain more data. This helps LSTMs overcome

some of the drawbacks of regular RNNs, namely the issue of vanishing and exploding gradients which arise from the recursive calculation of the gradients over the entries of the time series. In the problem of forecasting the displacements of a structure in fire, the history of both the displacement and temperature are crucial. This makes LSTMs, with their ability to learn the history of time series, an invaluable tool for the regression problem tackled in this paper. Readers interested in the mathematical implementations of recurrent networks and LSTMs are suggested to refer to some of the established textbooks on the topic such as [44] and chapter 5 of [45] for a more practical treatment.

Another of the distinct advantages of LSTM networks over traditional RNNs is their versatility in performing different types of mapping between inputs and outputs, including one-to-one, many-to-one, and many-to-many relationships. This is particularly useful because the displacement at any monitoring point depends on both the temperature and displacement at the current and nearby locations. At the system level, the displacement at any location is correlated with the displacements and temperatures at all other monitoring stations. This is particularly true for the cases with either no collapse or with global collapse. This has prompted other researchers to exploit the many-to-many mapping ability of LSTM networks to forecast the behaviour of a full structure [30]. The use of a single large LSTM network for many-to-many prediction has shown promise in terms of accuracy but raises challenges in terms of computational cost and flexibility. For example, training the two LSTM models in [30] needed 50,000 epochs which took over 30 hours in computational time for each. The required scale of the RNN for this many-to-many also means that if it were to be applied to a real structure with hundreds or even thousands of monitoring points, then the computational cost is likely to become infeasible. Moreover, in the case of a real fire, it is likely that some of the sensors in the structure would succumb to the fire or local failure and drop out of the network. This change in available input data would mean that the input into the large LSTM network architecture would need to either change, or the missing sensor data would need to be compensated for somehow. There is currently no simple solution to resolve this issue that would severely impact the robustness of the prediction system.

In this work, an alternative “modular AI” approach is used that mitigates these issues. Using modular AI in collapse prediction in fire involves breaking down the problem into smaller, more manageable “tasks” and using separate AI models, or “modules”, to address each task. For the reticulated aluminium structure in this study, each task is the prediction of displacement at a single key monitoring location. That is, each AI model only performs many-to-one mapping to forecast the displacements at only one location based on local conditions of displacement and temperature. In this way, each AI model is trained and optimized for the specifics of the local monitoring point such as connection details and material properties, leading to good predictions for this relatively simple regression problem. During the future full-scale experiment,

another set of modular AI models for forecasting the temperatures of the fire at each location would also be deployed based on the work of Zhang et al. [46]. These modules would generate a constant stream of "true" fire temperatures that would be used by the displacement forecasting modules.

The division of tasks into temperature and displacement forecasting at only local positions allows for easier maintenance and updating of the individual models, and flexibility to adapt to changes in the structure and in the available sensors. More importantly, each modular model is both simple and uses only a few parameters, thus resulting in only a small number of epochs being necessary for training. When it comes to forecasting in a real fire, each model is deployed independently as a part of a large internet of things network. This means that the overall system is rather robust to loss of sensors as such losses only affect a handful of local models, whose loss of output is in its own right a data point on the state of the structure.

6.2 Architecture, Training, and Forecasting

The individual AI models were built in PyTorch with the architecture as shown in Fig. 18. Each model takes a number of time series each representing one of the features that are used for forecasting. That is, each time series represents the past displacements or temperatures around the monitoring point the AI model is intended to forecast for. For example, the model for forecasting the displacements at monitoring point 5 would take the previous displacements at this point as well as the temperatures at temperature points 7 and 8, which surround it. As shown in **Fig. 17**, the features used in this example includes the displacement data from the displacement monitoring point 5 and the temperatures from the two nearby temperature monitoring points 7 and 8. The output is the prediction of future displacement at displacement monitoring point 5. In this model, displacement point 5 has been singled out as a representative indicator of the structural integrity of the entire structure. Consequently, the categorisation of collapse and no collapse states have been adjusted while maintaining alignment with the theoretical premise of critical displacement -0.5 m. When the displacement at displacement monitoring point 5 exceeds the critical value of -0.5 m, the case is classified as a collapse case. Otherwise, the cases are classified as no collapse cases.

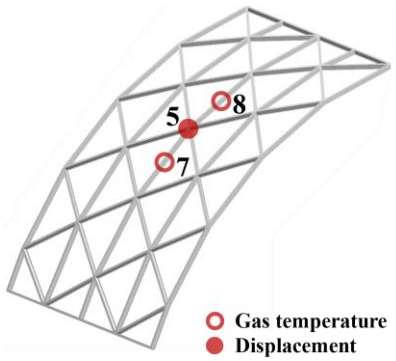

Fig. 17 An example of selected monitoring points for individual LSTM model training.

The inputs are passed to an LSTM layer with a hidden state of size 64. The output of this layer is fed into a fully connected layer and then an activation function (LeakyReLU). The output of the LeakyReLU activation is passed to a final fully connected output layer. Training is performed in minibatches of 64 sequences. Each minibatch consist of a window of 40 points, and a label of a single point representing the next point in the sequence. However, because each OpenSees simulation had a separate time scale and a unique number of points, an interpolation step was performed before training so that all time series would have exactly 200 points. The output of the 960 OpenSees simulations and fire data discussed in the previous sections were divided into a 60%, 20%, and 20% training, testing, and validation subsets, respectively. The series were randomly shuffled, and their minimum and maximum values were calculated separately to prevent data leakage. Min-max scaling was applied to the input features so that the temperatures and displacements would all be limited to the range between 0 and 1. This was done to prevent the difference in scale between the displacement and temperatures from skewing the training and forecasting processes. The Adam optimiser and the mean square error loss function were used for training, and the hidden state of the LSTM layer was initialised to zero at each epoch. Training was performed for only 50 epochs which was sufficient to produce very good results while reducing the risk of overfitting to the training data.

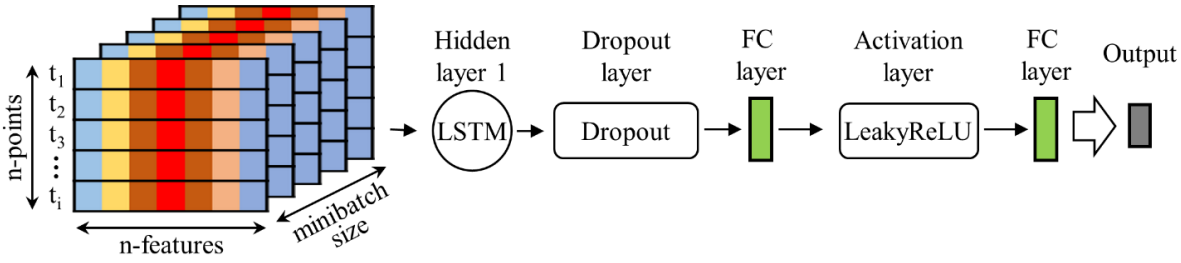

Fig. 18 Architecture of the modular AI models.

After the training phase, the forecasting process was performed in three batches each of which encompassed all time series from the training, testing, and validation subsets, respectively. This approach was taken to make the forecasting process computationally efficient and to simplify post processing of the results. During the forecasting phase, an initial window of 40 points of each feature was fed to the model which used this data to predict the displacement at the local monitoring point for the next time step. This process was repeated recursively, with the predicted data appended to the provided input sequence. The utilisation of a simple and small LSTM model for prediction made this process computationally inexpensive but came with additional caveats that will be discussed in section 6.4.

6.3 AI Models for Global Predictions

Upon analysing the OpenSees simulation data, it was observed that the displacements of the monitoring points at locations 4 and 5 were often some of the first and most prominently indicative of global collapse,

as evidenced in **Fig. 12**. As such, it is feasible to use a single AI model for forecasting the performance at location 5 as a surrogate for the state of the entire structure. An AI module was trained for this monitoring point based on the previous displacement and temperatures at the two nearby temperature monitoring points 7 and 8.

Fig. 19 (a), (b), and (c) shows the prediction of the AI model for a case associated with failure, partial failure, and no failure, respectively. For these particular validation scenarios, the AI module was able to produce a good forecast of the behaviour. It is able to predict the increase in deflection with very good accuracy, and was also able to capture that the case associated with partial collapse had some noticeable deflection, although it failed to predict the vibrations in the deflection. In the case of **Fig. 19** (c), the model also predicted that the deflections would be very small.

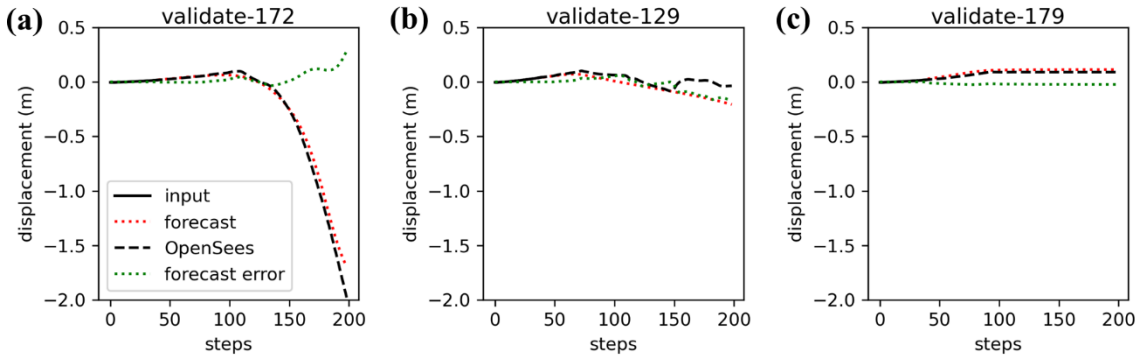

Fig. 19 AI module forecast for some of the fire/simulation cases that were predicted well.

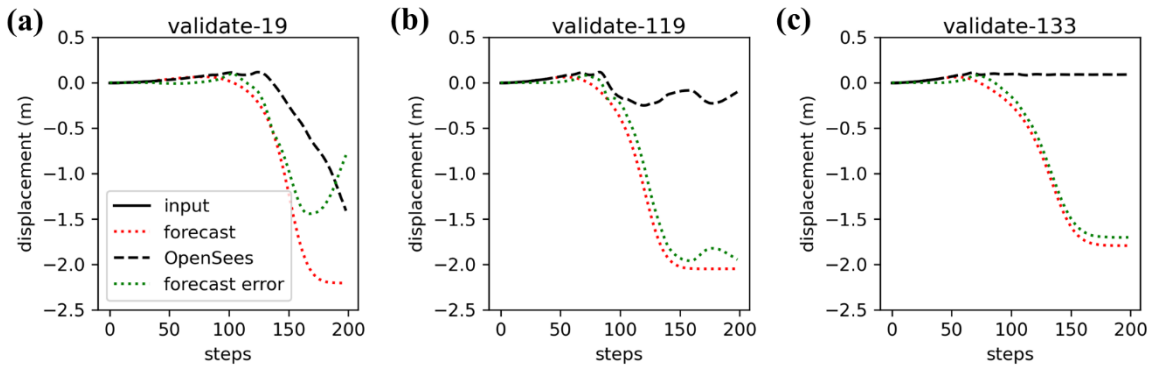

Fig. 20 AI module forecast for some of the fire/simulation cases that were predicted poorly.

Fig. 20 (a), (b), and (c) shows cases that the AI model was unable to predict very well. In all these cases, the AI module predicted that the monitoring point at location 5 would encounter runaway deflections that are indicative of collapse. In the case of **Fig. 20** (a) where collapse actually occurred, the AI module predicted early runaway failure. The minor vibrations associated with partial collapse shown in **Fig. 20** (b) were also overestimated and predicted as very large deflections. Likewise, false collapse was also predicted

the case of **Fig. 20** (c) where the OpenSees deflections were minimal and associated with a fire that did not severely impact structural stability.

Assuming that any deflections at monitoring point 5 beyond 0.5 m are associated with collapse, then the AI model has a combined testing and validation collapse sensitivity of 96%. It also has precision of 70% (70% of predicted collapse cases are true collapse cases). This means that while it is unlikely that the model would miss a scenario where collapse would occur, it is also likely to predict that a benign fire exposure would devolve into runaway deflections. The error matrix is shown in **Table 2**, and explains how the model performs for collapse and no collapse.

Table 2 Error Matrix for forecasting at location 5.

	Predicted collapse	**Predicted no collapse**
True collapse	202	8
True no collapse	84	666

While this case of high sensitivity is very important for smart firefighting because it ensures sounding the warning alarm for firefighters, it results in a distribution of errors that makes it difficult to judge the efficacy of the AI model. **Fig. 21** showcases the distribution of mean error (the difference in magnitude between the true and forecasted points divided by number of points). The mean and median of the combined testing and validation mean errors are -0.011 m and 0.028 m respectively. Of course, these values are skewed by the large errors that arise from predicting large deflections when the structure is stable, as shown by the tails of the distribution.

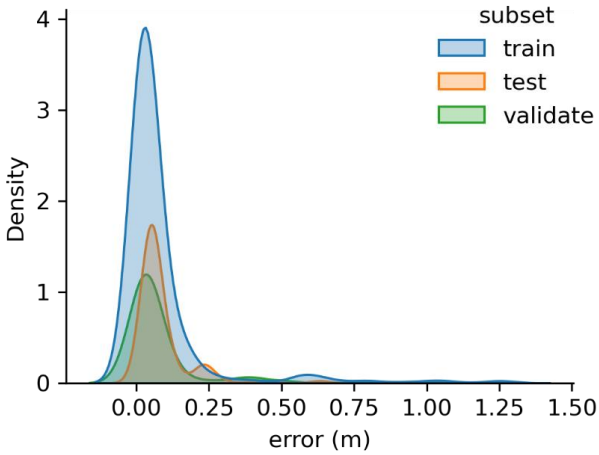

Fig. 21 Distribution of the mean error for the forecast at monitoring point 5.

An important feature of using AI for real-time forecasting of displacements is that the predictions get better when more data is provided. In the results presented so far, the forecasts were all generated with only 20%

of the sequence provided as input. **Fig. 22** shows how the accuracy of the prediction changes with more data provided as input. The more data is provided, the closer some forecasts are to the OpenSees simulation output.

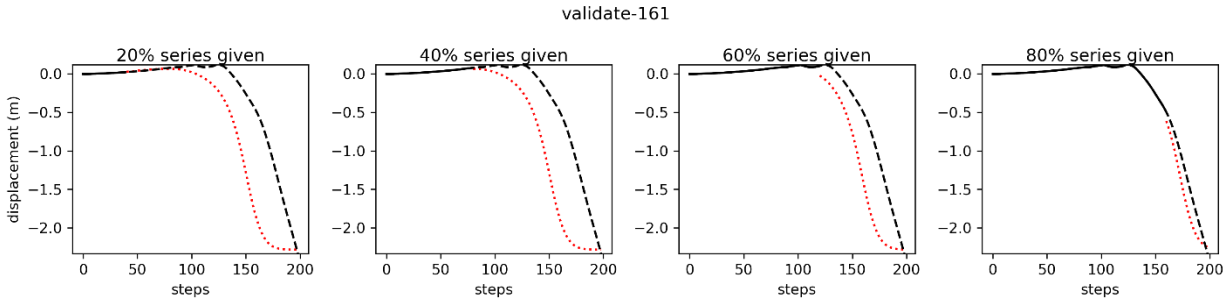

Fig. 22 Change in forecasting validity with change in number of provided data points.

6.4 Limitations

While the modular AI approach reduces the computational cost of training a large model, it also comes with its own set of challenges. Even though each AI module is lightweight and very quick to train, there are simply too many of them for a real structure. Even for the relatively small-scale problem of the reticulated aluminium roof, training and fine-tuning 8 separate models involves a significant amount of personnel overhead. Trying to train all the models with the same hyper parameters inevitably leads to discrepancies in the accuracy between the models as shown in **Fig. 23**.

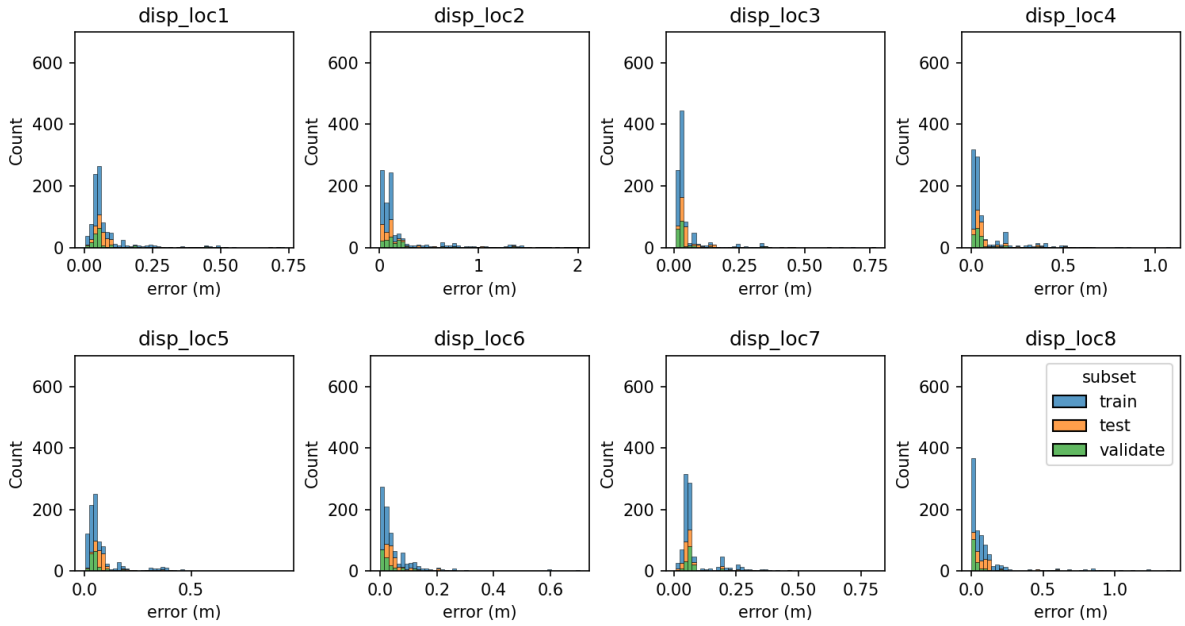

Fig. 23 Discrepancies in accuracy between models when training all of them using the same hyper parameters.

This figure shows the absolute value of the mean error for the forecast of each sequence. All modules were trained with the same hyper parameters that performed well for the module used to forecast the displacements at monitoring point 5. For a real building with hundreds or thousands of monitoring points, it is likely not possible to manually finetune the hyper parameters of each AI module, and an automation process is definitely needed. While Fig. 23 and the mean and median of the shown distributions may offer some picture of the performance of the AI modules, it is believed that the sensitivity and precision in predicting collapse would be better indicators of model performance when training many AI models concurrently.

Additionally, each AI module is only concerned with the local past deflections and local temperatures. As explained earlier, however, the features at the neighbouring monitoring points can influence one another. Using only the local features overlooks this completely and can result in strange results where one model could predict collapse while another forecasts that the structure would undergo very low deflections. In future work, the authors aim to remedy this issue by requiring that the AI modules at the neighbouring points communicate with one another and share information during the forecasting process.

A final point to note in this section is that despite covering the range of expected structural behaviours by relying on a large number of fire sizes and models, there was no explicit consideration of the variation in material properties or imperfections in the construction. This means that even though it is expected that the AI models would be able to recognize a potential collapse mechanism, for example, it may not be able to do so with the same fidelity if it occurs at lower temperatures due to worse material properties than modelled.

7. Conclusions

This paper proposed and implemented a modular AI approach for real-time forecasting of the displacements at monitoring points in a large structure. This approach aims to reduce the computational demands that large AI models would require when forecasting global behaviour, as well as simplify the deployment process for large structures. While this paper has shown that this approach is feasible and can produce reliable predictions that are sensitive to collapse, it has also shown that there are still some unresolved issues that need to be tackled. While each model is very inexpensive to train, the large number of models required for a real structure necessitates automating the training and hyperparameter tuning processes. It was shown in this paper that if each model is not fine tuned for the local conditions it is hoping to forecast for, then the global predictions may suffer as each model would have different levels of accuracy. Relative error was found to not be a very good indicator of model behaviour because it punishes the large errors introduced by forecasting failure when the structural performance is actually stable. In smart firefighting, sensitivity to failure should prioritized over precision as it ensures that the AI system is more likely to warn firefighters

in the case of impending collapse. A false warning when no failure takes place is acceptable, but no warning before failure is not. Future work will focus on improving the global forecast network by allowing neighbouring modules to communicate. Moreover, in light of the upcoming experiment to take place in SCFRI, future work will also include enriching the modelling database with more fire scenarios, as well as automating the training of the AI modules so that each of them would have a sufficient level of sensitivity and precision.

Acknowledgements

This work is funded by the Hong Kong Research Grants Council Theme-based Research Scheme (T22-505/19-N).

References

[1] R.G. Gann, A. Hamins, K. McGrattan, H.E. Nelson, T.J. Ohlemiller, K.R. Prasad, W.M. Pitts, Reconstruction of the Fires and Thermal Environment in World Trade Center Buildings 1, 2, and 7, Fire Technology. 49 (2013) 679–707. https://doi.org/10.1007/s10694-012-0288-3.

[2] I. Fletcher, A. Borg, N. Hitchen, S. Welch, Performance of concrete in fire: A review of the state of the art, with a case study of the Windsor Tower fire, 4th International Workshop in Structures in Fire. (2006) 779–790.

[3] B. Meacham, H. Park, I.J. Straalen, Fire and Collapse , Faculty of Architecture Building , Delft University of Technology : Data Collection and Preliminary Analyses, Architecture. (2008) 14.

[4] T. Yarlagadda, H. Hajiloo, L. Jiang, M. Green, A. Usmani, Preliminary modelling of Plasco Tower collapse, International Journal of High-Rise Buildings. 7 (2018) 397–408. https://doi.org/10.21022/IJHRB.2018.7.4.397.

[5] M.A. Khan, A.A. Khan, A.S. Usmani, X. Huang, Can fire cause the collapse of Plasco Building: A numerical investigation, Fire and Materials. 46 (2022) 560–575. https://doi.org/10.1002/fam.3003.

[6] CNN Editorial Research, September 11 Terror Attacks Fast Facts, CNN. (2015).

[7] N. Johansson, S. Svensson, Review of the Use of Fire Dynamics Theory in Fire Service Activities, Fire Technology. 55 (2019) 81–103. https://doi.org/10.1007/s10694-018-0774-3.

[8] K. Prasad, H.R. Baum, Coupled fire dynamics and thermal response of complex building structures, in: Proceedings of the Combustion Institute, 2005: pp. 2255–2262. https://doi.org/10.1016/j.proci.2004.08.118.

[9] C. Zhang, J.G. Silva, C. Weinschenk, D. Kamikawa, Y. Hasemi, Simulation Methodology for Coupled Fire-Structure Analysis: Modeling Localized Fire Tests on a Steel Column, Fire Technology. 52 (2016) 239–262. https://doi.org/10.1007/s10694-015-0495-9.

[10] J.C.G. Silva, A. Landesmann, F.L.B. Ribeiro, Fire-thermomechanical interface model for performance-based analysis of structures exposed to fire, Fire Safety Journal. 83 (2016) 66–78. https://doi.org/10.1016/j.firesaf.2016.04.007.

[11] D. Woo, J.K. Seo, Numerical validation of the two-way fluid-structure interaction method for non-linear structural analysis under fire conditions, Journal of Marine Science and Engineering. 9 (2021). https://doi.org/10.3390/jmse9040400.

[12] A.A. Khan, M.A. Khan, C. Zhang, L. Jiang, A. Usmani, OpenFIRE: An Open Computational Framework for Structural Response to Real Fires, Fire Technology. 58 (2022) 1011–1038.

https://doi.org/10.1007/s10694-021-01184-0.

[13] M.A. Orabi, A.A. Khan, L. Jiang, T. Yarlagadda, J. Torero, A. Usmani, Integrated nonlinear structural simulation of composite buildings in fire, Engineering Structures. 252 (2022). https://doi.org/10.1016/j.engstruct.2021.113593.

[14] R.K. Janardhan, S. Shakil, W. Lu, S. Hostikka, J. Puttonen, Coupled CFD-FE analysis of a long-span truss beam exposed to spreading fires, Engineering Structures. 259 (2022) 114150. https://doi.org/10.1016/j.engstruct.2022.114150.

[15] J. Jiang, Y. Lu, X. Dai, G.Q. Li, W. Chen, J. Ye, Disproportionate collapse of steel-framed gravity buildings under travelling fires, Engineering Structures. 245 (2021) 112799. https://doi.org/10.1016/j.engstruct.2021.112799.

[16] J. Stern-gottfried, G. Rein, Travelling fires for structural design – Part I : Literature review, Fire Safety Journal. 54 (2012) 74–85. https://doi.org/10.1016/j.firesaf.2012.06.003.

[17] X. Dai, S. Welch, A. Usmani, A critical review of "travelling fire" scenarios for performance-based structural engineering, Fire Safety Journal. 91 (2017) 568–578. https://doi.org/10.1016/j.firesaf.2017.04.001.

[18] Z. Nan, X. Dai, H. Chen, S. Welch, A. Usmani, A numerical investigation of 3D structural behavior for steel-composite structures under various travelling fire scenarios, Engineering Structures. (n.d.). https://doi.org/10.14264/a1068ab.

[19] L. Han, S. Potter, G. Beckett, G. Pringle, S. Welch, S.H. Koo, G. Wickler, A. Usmani, J.L. Torero, A. Tate, FireGrid: An e-infrastructure for next-generation emergency response support, Journal of Parallel and Distributed Computing. 70 (2010) 1128–1141. https://doi.org/10.1016/j.jpdc.2010.06.005.

[20] X. Wu, Y. Park, A. Li, X. Huang, F. Xiao, A. Usmani, Smart Detection of Fire Source in Tunnel Based on the Numerical Database and Artificial Intelligence, Fire Technology. 57 (2021) 657–682. https://doi.org/10.1007/s10694-020-00985-z.

[21] X. Wu, X. Zhang, X. Huang, F. Xiao, A. Usmani, A real-time forecast of tunnel fire based on numerical database and artificial intelligence, Building Simulation. 15 (2022) 511–524. https://doi.org/10.1007/s12273-021-0775-x.

[22] T. Zhang, Z. Wang, Y. Zeng, X. Wu, X. Huang, F. Xiao, Building Artificial-Intelligence Digital Fire (AID-Fire) system: A real-scale demonstration, Journal of Building Engineering. 62 (2022) 105363. https://doi.org/10.1016/J.JOBE.2022.105363.

[23] L. chu Su, X. Wu, X. Zhang, X. Huang, Smart performance-based design for building fire safety: Prediction of smoke motion via AI, Journal of Building Engineering. 43 (2021) 102529. https://doi.org/10.1016/j.jobe.2021.102529.

[24] A.A. Khan, M.A. Khan, K. Leung, X. Huang, M. Luo, A. Usmani, A review of critical fire event library for buildings and safety framework for smart firefighting, International Journal of Disaster Risk Reduction. 83 (2022) 103412. https://doi.org/10.1016/j.ijdrr.2022.103412.

[25] M.Z. Naser, Mechanistically Informed Machine Learning and Artificial Intelligence in Fire Engineering and Sciences, Fire Technology. 57 (2021) 2741–2784. https://doi.org/10.1007/s10694-020-01069-8.

[26] F. Fu, Fire induced progressive collapse potential assessment of steel framed buildings using machine learning, Journal of Constructional Steel Research. 166 (2020). https://doi.org/10.1016/j.jcsr.2019.105918.

[27] Z. Ye, S.C. Hsu, H.H. Wei, Real-time prediction of structural fire responses: A finite element-based machine-learning approach, Automation in Construction. 136 (2022) 104165. https://doi.org/10.1016/j.autcon.2022.104165.

[28] Z. Ye, S.C. Hsu, Predicting real-time deformation of structure in fire using machine learning with CFD and FEM, Automation in Construction. 143 (2022) 104574. https://doi.org/10.1016/j.autcon.2022.104574.
[29] S. Hochreiter, J. Schmidhuber, Long short-term memory, Neural Computation. 9 (1997) 1735–1780.
[30] W. Ji, G.-Q. Li, S. Zhu, Real-time prediction of key monitoring physical parameters for early warning of fire-induced building collapse, Computers & Structures. 272 (2022) 106875. https://doi.org/10.1016/j.compstruc.2022.106875.
[31] W. Ji, G.Q. Li, G.B. Lou, Early-warning methods for fire-induced collapse of single span steel portal frames, Journal of Constructional Steel Research. 190 (2022) 107154. https://doi.org/10.1016/j.jcsr.2022.107154.
[32] BS EN 1991-1-2:2002. Eurocode 1: Actions of Structures - Part 1-2: General Actions - Actions on Structures Exposed to Fire., 2002.
[33] Y. Jiang, Development and application of a thermal analysis framework in OpenSees for structures in fire, The University of Edinburgh, 2012.
[34] L. Jiang, Development of an integrated computational tool for modelling structural frames in fire considering local effects, The University of Edinburgh, 2015.
[35] M.A. Orabi, A.A. Khan, A. Usmani, An Overview of OpenSEES for Fire, in: Proceedings of the 1st Eurasian Conference on OpenSEES: OpenSEES Days Eurasia, Hong Kong, China, 2019.
[36] F.M. Mazzolani, EN1999 Eurocode 9: Design of aluminium structures, in: Proceedings of the Institution of Civil Engineers-Civil Engineering, Thomas Telford Ltd, 2001: pp. 61–64.
[37] E. Rackauskaite, P. Kotsovinos, A. Jeffers, G. Rein, Structural analysis of multi-storey steel frames exposed to travelling fires and traditional design fires, Engineering Structures. 150 (2017) 271–287. https://doi.org/10.1016/j.engstruct.2017.06.055.
[38] J. Jiang, G.-Q. Li, Disproportionate collapse of 3D steel-framed structures exposed to various compartment fires, Journal of Constructional Steel Research. 138 (2017) 594–607. https://doi.org/10.1016/j.jcsr.2017.08.007.
[39] M.A. Orabi, L. Jiang, A. Usmani, J. Torero, The Collapse of World Trade Center 7: Revisited, Fire Technology. (2022). https://doi.org/10.1007/s10694-022-01225-2.
[40] Y. Hasemi, Y. Yokobayashi, T. Wakamatsu, A. V. Ptchelintsev, Modelling of heating mechanism and thermal response of structural components exposed to localised fires.Thirteenth Meeting of the UJNR Planel on Fire Research and Safety, 1996.
[41] Z. Nan, A.A. Khan, L. Jiang, S. Chen, A. Usmani, Application of Travelling Behaviour Models for Thermal Responses in Large Compartment Fires, Fire Safety Journal. (n.d.) 1–30.
[42] M. Law, The origins of the 5 MW design fire, Fire Saf Eng. 2 (1995) 343–346.
[43] NFPA® 92B, Standard for Smoke Management Systems in Malls , Atria , and Large Spaces, 2009.
[44] F.M. Bianchi, E. Maiorino, M.C. Kampffmeyer, A. Rizzi, R. Jenssen, Recurrent Neural Networks for Short-Term Load Forecasting, Springer International Publishing, Cham, 2017. https://doi.org/10.1007/978-3-319-70338-1.
[45] I. Pointer, PyTorch for Deep Learning, n.d.
[46] T. Zhang, Z. Wang, H.Y. Wong, W.C. Tam, X. Huang, F. Xiao, Real-time forecast of compartment fire and flashover based on deep learning, Fire Safety Journal. 130 (2022) 103579. https://doi.org/10.1016/j.firesaf.2022.103579.